Optical Materials 32 (2009) 311–314

Contents lists available at ScienceDirect

Optical Materials

journal homepage: www.elsevier.com/locate/optmat

Crystal growth, optical properties, and α-ray responses of Ce-doped $LiCaAlF_6$ for different Ce concentration

Takayuki Yanagida [a,*], Akira Yoshikawa [a,b], Yuui Yokota [a], Shuji Maeo [a], Noriaki Kawaguchi [c], Sumito Ishizu [c], Kentaro Fukuda [c], Toshihisa Suyama [c]

[a] Institute of Multidisciplinary Research for Advanced Materials, Tohoku University, 2-1-1 Katahira, Aoba-ku, Sendai 980-8577, Japan
[b] New Industry Creation Hatchery Center (NICHe), Tohoku University, 6-6-10 Aoba, Aramaki, Aoba-ku, Sendai 980-8579, Japan
[c] Tokuyama Corporation Shibuya 3-Chome, Shibuya-ku, Tokyo 150-8383, Japan

ARTICLE INFO

Article history:
Received 22 May 2009
Received in revised form 30 July 2009
Accepted 17 August 2009
Available online 22 September 2009

PACS:
07.57.K
78.60.Y
78.20

Keywords:
Fluoride
Single crystal
Crystal growth from the melt
Ce^{3+}
Radiation
Scintillator
Neutron

ABSTRACT

Ce 1%, 2%, and 3%-doped $LiCaAlF_6$ (LiCAF) single crystals were grown by the micro-pulling-down method. The crystals were transparent, 2.0 mm in diameter and 30–60 mm in length. Neither visible inclusions nor cracks were observed. Optical properties, including absorption coefficient, and photoluminescence emission spectra were measured. The strong absorption line was observed at 260 nm, and absorption coefficients of this line were proportional to Ce^{3+} concentration. Emission due to Ce^{3+} 5d–4f transition peaking around 285 nm and 310 nm were observed by 260 nm excitation. Simulating a neutron irradiation, ^{241}Am 5.5 MeV α-ray was used to excite the samples. After a correction of a quantum efficiency of photomultiplier tube and compared with Li–glass scintillator GS20, light yield of 6600 ph/n, and 41 ns decay were achieved 3% doped.

1. Introduction

Ce^{3+} doped fluoride have been studied for many years for their UV emissions for scintillator [1,2] and all-solid-state tunable laser applications [3]. Especially, an intense study has been made in Ce-doped Colquiriite-type fluoride single crystals such as $LiCaAlF_6$ (Ce:LiCAF) and $LiSrAlF_6$ (Ce:LiSAF) as leading candidates for tunable all-solid-state lasers in the UV wavelength region [4,5]. The emission is due to parity-allowed radiative transitions from the lowest level of the excited 4f5d configuration to 4f ground levels of $^2F_{7/2}$ and $^2F_{5/2}$ states of Ce^{3+}. In recent years, Li-containing fluorides are under study to provide new scintillation materials for neutron detection due to the high cross-section of ^6Li for neutron capture. Once a neutron is captured by ^6Li in the scintillator, the reaction such as $^6Li + n \rightarrow \alpha + {}^3H + 4.78$ MeV occurs and generates alpha and triton particles which excite the host lattice of the scintillator. For thermal neutron detection, Li–glass scintillator has played a major role [6–8], because its medium light yield (6000 ph/n) and fast decay (75 ns) are very attractive points for applications. But the weak points of Li–glass scintillators are high cost and the poor carrier mobilities, due to the intrinsically less-ordered structure, compared to single crystals, limiting their light yields. In order to develop a new candidate for thermal neutron detection, as the first step, we developed Ce 0.5% doped LiCAF scintillator by the micro-pulling-down (μ-PD) method, and investigated its optical and radiation properties [9]. When it was excited by ^{241}Am α-ray, the emission peak appeared at approximately 300 nm. By an excitation by ^{252}Cf neutrons, Ce 0.5% LiCAF exhibited a light yield of 4200 ph/n and a decay time constant of 38 ns [9]. This result confirmed that Ce:$LiCaAlF_6$ could be applied for neutron detectors.

Recent establishment of the μ-PD method for the growth of fluoride systems [10] allow us the systematic study of fluorides with different dopant concentration. The present work provides basic properties of Ce:LiCAF for different Ce concentration. By utilizing the μ-PD method, we have developed Ce^{3+} 1%, 2%, and

* Corresponding author. Tel.: +81 22 217 5822; fax: +81 22 217 5102.
E-mail address: t_yanagi@tagen.tohoku.ac.jp (T. Yanagida).

0925-3467/$ - see front matter © 2009 Elsevier B.V. All rights reserved.
doi:10.1016/j.optmat.2009.08.007

3%-doped LiCAF single crystals. To investigate optical characteristics of these crystals, we studied their absorption coefficient, emission spectra, and photoluminescence decay. Finally, in order to investigate scintillation properties, including the light yield and the decay curve, we measured α-ray responses of these crystals, by ^{241}Am irradiation, imitating the neutron irradiation.

2. Experimental procedure

Nominal compositions $Li(Ca_{1-x}Ce_x)AlF_6$ (x = 0.01, 0.02, and 0.03) single crystals were grown using 4 N LiF, CaF_2, AlF_3, CeF_3 powders (Stella Chemifa Co. Ltd.) as starting materials. Crystal growth was carried out by the μ-PD method with graphite crucible under Ar + CF_4 atmosphere after baking of starting materials, crucible, heater, insulator and so on under high vacuum (<10^{-4} Pa) to prevent contamination of oxygen. Tungsten–rhenium wire was used instead of the seed for the crystal growth and the crystal growth rate was approximately 0.1 mm/min. The typical thermal setup and the baking procedure for fluoride crystal growth were reported in Ref. [10].

Transmittance were obtained at spectrofluorometer (JASCO, V550), and reflectance were measured by the other spectrofluorometer (Shimadzu UV2550). By synthesizing of these spectra and the thickness of our sample, absorption coefficient was obtained. The photoluminescence spectra were obtained by using Edingburgh FLS920. The step in the spectra acquisition was set to be 1 nm at each measurement, and all the measurements were carried out at room temperature. By 260 nm excitation, photoluminescence decay was also studied.

By using a PMT (Hamamatsu R7600, 18 × 18 mm^2 square window), we measured the light yield (LY) of the three LiCAF crystals when excited by α-rays, in comparison with a Li–glass GS20 scintillator. The reason why we used α-ray was to imitate the reaction ^{6}Li(n, α)^{3}H. Thus, ^{241}Am α-ray source which emitted 5.5 MeV α-ray was used in this experiment. We mounted each crystal on the PMT with a silicon grease (OKEN, 6262 A). When α-ray was detected, the signals are fed into a preamplifier (ORTEC, 9306), a shaping-amplifier (ORTEC, 572), a multichannel analyzer (hereafter MCA, AmpTec 8000 A), and finally to a personal computer (PC). We applied high voltage (HV) of −700 V to the PMT, and employed a shaping time of 0.5 μsec.

3. Result and discussion

3.1. Crystal elaboration

As-grown crystal rods of $Li(Ca_{1-x}Ce_x)AlF_6$ (x = 0.01, 0.02, and 0.03) had around 2.0 mm in diameter and 40–50 mm in length and all the crystals were transparent. There were neither visible inclusions nor cracks in the crystals. The plate-like crystal, which was cut from as-grown crystal rod was shown in Fig. 1. Although EPMA (Electron Probe Micro Analyzer) analysis was done to determine the actual Ce concentration, the actual value was unknown implicating very tiny (<0.1 mol%) Ce activation. As a view of ion radius, Ce^{3+} ion could substitute for Ca^{2+}, but a charge compensation of Ca^{2+} site and Ce^{3+} ion prevented us from a large amount of substitution. The dimensions of plate-like crystals were 1 × 2 × 9 mm^3, 1 × 2 × 8 mm^3, and 1 × 2 × 15 mm^3 for Ce 1%, 2%, and 3%, respectively. The wide surfaces of crystals were polished and they were used for the optical experiments.

3.2. Spectroscopic characterization

Absorption spectra are shown in Fig. 2, where the absorption line around 260 nm of LiCAF corresponds with absorption of

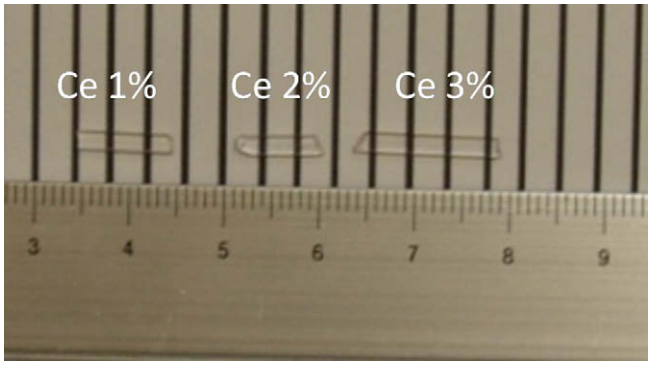

Fig. 1. Photograph of cut and polished Ce-doped $LiCaAlF_6$ (LiCAF) single crystals grown by the μ-PD method. From left to right, nominal concentrations of Ce are 1, 2, and 3 mol%.

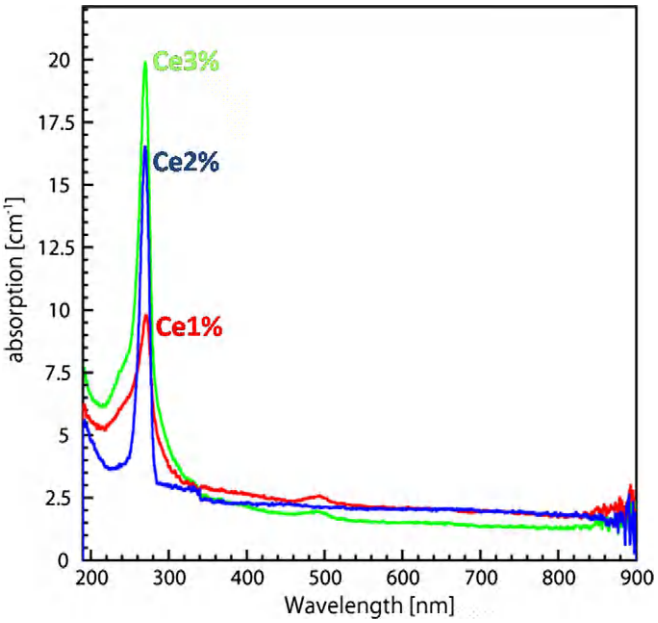

Fig. 2. Absorption coefficient (cm^{-1}) of Ce^{3+} doped LiCAF single crystals plotted against the wavelength. Red, blue, and green represents Ce 1%, 2%, and 3%, respectively (For interpretation of the references to colour in this figure legend, the reader is referred to the web version of this article.).

Ce^{3+}. Different absorption amplitude at 260 nm in these crystals is attributed to actual Ce^{3+} concentrations, and is proportional to Ce^{3+} concentration. Although the intrinsic absorption of LiCAlF itself due to some defects appeared in the same region [11], this proportional relation confirmed that this absorption was caused by Ce^{3+}.

Previous studies indicated that the intrinsic emission of non-doped $LiCaAlF_6$ grown by the Czochralski technique appears at 280 nm due to STE [11]. This line is very broad with a half-width of approximately 100 nm and it does not show up in the room temperature. The same authors also investigate Ce^{3+} emission in LiCAF host, and two lines at 285 nm and 310 nm are observed which overlaps in the intrinsic emission range [12]. They argued the origin of the emission of Ce:LiCAF as the radiative 5d–4f transitions in unperturbed Ce^{3+} ion replacing Ca^{2+} ion in octahedral site. However, the other authors explained that the former line (285 nm) is a regular emission and the latter (310 nm) "perturbed" emission from Ce^{3+}, because the experimental results of Ce^{3+} doped CaF_2 showed the separation of the two peaks in the emission spectrum was too high to be explained by the usually considered 4f ground

level splitting of Ce^{3+} [13]. Additionally, it should be noted that they used the same manufacturing source of the crystal (possibly cut from the same ingot), and except a small part of results, the measured crystal was not Ce:LICAF but Ce–Na co-doped LiCAF.

To clarify the nature of the emission of Ce:LiCAF is far beyond from the purpose of the present work, we adopt usual interpretation from our experimental results. Fig. 3 shows emission spectra excited by 260 nm photons, where emission due to Ce^{3+} 5d–4f related transition peaking around 285 nm and 310 nm were detected. A weak peak at 340 nm was observed in 1% and 2% crystals. As the Ce concentration is increased, the intensity of this peak becomes weaker, which is a general feature of intrinsic emissions. In the same figure, emission spectrum of non-doped LiCAF grown by the μ-PD method is superposed to study the nature of the 340 nm line. There are weak lines at 340 nm and 370 nm observed. From this result, a broad line around 340 nm in Ce-doped crystals will be attributed to an intrinsic emission from LiCAF itself and also the 370 nm line will be the intrinsic emission by the same consideration. Although the past result exhibited that the intrinsic emission only appeared in low temperature [12], the discrepancy with the present result may be attributed to a difference of a growth technique, because the crystallinity of the μ-PD grown crystal is generally worse than that of the Czochralski grown one. The other possibility is an effect of co-doped Na^{+} ions in past results. In spite of the smallest sample size, the 2% doped one resulted the highest emission intensity. A very weak line around 390 nm is an artifact of our experimental setup.

Photoluminescence decay curves are represented in Fig. 4. There are very little differences in three LiCAFs. By a single exponential fitting with a deconvolution of instrumental responses, we obtained 26 ns as a decay time for all the LiCAFs, which is consistent with the other results reported as 25 ns [11].

3.3. α-ray responses

To simulate a neutron irradiation, we irradiated 5.5 MeV α-ray from ^{241}Am, and compared the pulse height with a reference Li–glass GS20 scintillator. Fig. 5 represents pulse height spectra of Ce:-LiCAFs and GS20. As shown in this figure, GS20 shows the highest pulse height peaking around 600 ch, and the second highest pulse height is achieved by the Ce 3% doped one. In 1% and 2% doped samples, there were two peak channels identified. This phenomenon is likely due to agglomeration of Ce^{3+} in LiCAF host generated during the growth process, and regions with higher Ce concentration and lower Ce concentration produce the two different pulse heights. From EDS analysis, we actually detected regions where the Ce concentration is higher than others. In case Ce doping level is too high, high-Ce-concentration regions will be created in the crystal, because excessive Ce cannot be discharged to melt.

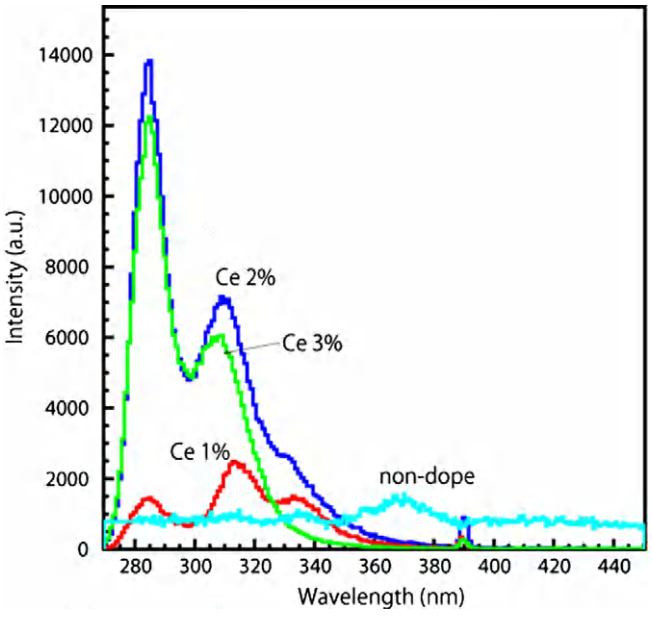

Fig. 3. Photoluminescence spectra of Ce^{3+} doped LiCAF single crystals excited by 260 nm photons. Red, blue, and green represents Ce 1%, 2%, and 3%, respectively. (For interpretation of the references to colour in this figure legend, the reader is referred to the web version of this article.)

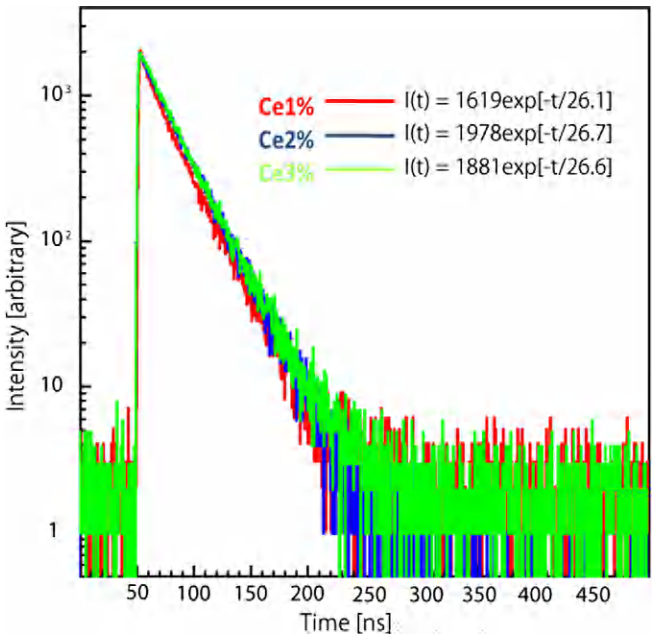

Fig. 4. Photoluminescence decay curves of Ce^{3+} doped LiCAF single crystals excited by 260 nm photons. Red, blue, and green represents Ce 1%, 2%, and 3%, respectively (For interpretation of the references to colour in this figure legend, the reader is referred to the web version of this article.).

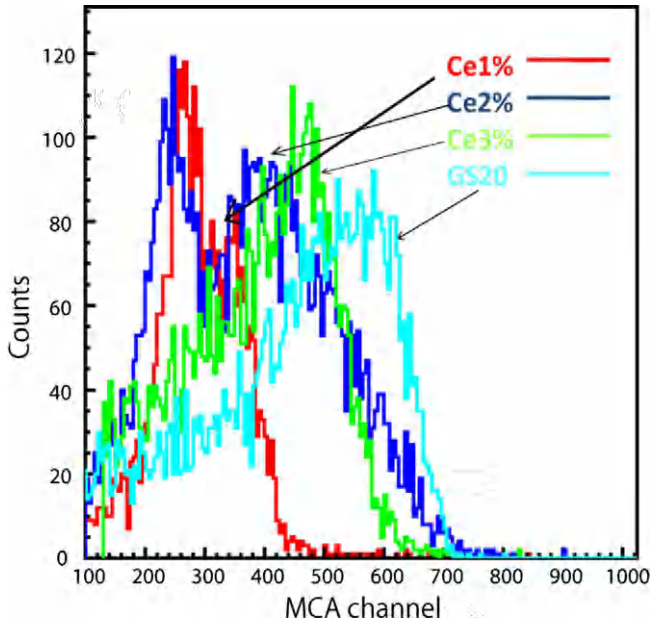

Fig. 5. ^{241}Am α-ray excited pulse height spectra of Ce^{3+} doped LiCAF single crystals and Li–glass Gs20. Red, blue, green, and cyan represents Ce 1%, 2%, 3%, and GS20 respectively (For interpretation of the references to colour in this figure legend, the reader is referred to the web version of this article.).

In our PMT, *QE* around 400 nm is 45% and around 300 nm 35%, respectively. Then we show a rough estimation of the light yield of our samples, by compared with GS20 (6000 ph/n, [6]). For example, the peak channel of 3% one was around 450 ch, and the light yield is calculated as 6000 [ph/n] × 452 ch/529 ch × 45%/35% = 6600 ph/n. Fig. 6 represents the light yield as a function of Ce concentration. In this calculation, we used the higher peak channel for 1% and 2% samples. From this result, if we could dope higher Ce^{3+} into $LiCaAlF_6$ lattice, more intense light yield will be expected.

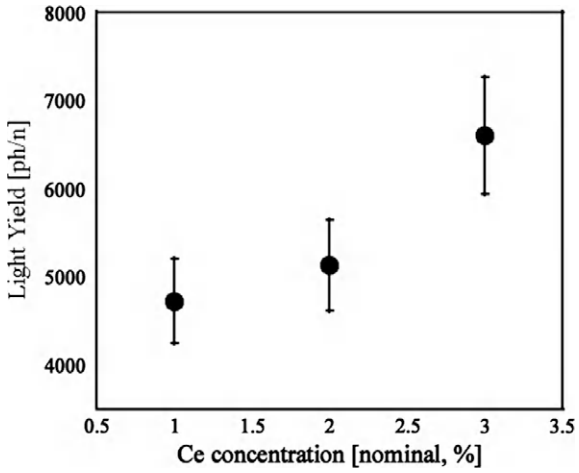

Fig. 6. Light yield (ph/n) plotted against the Ce concentration by ^{241}Am α-ray irradiation.

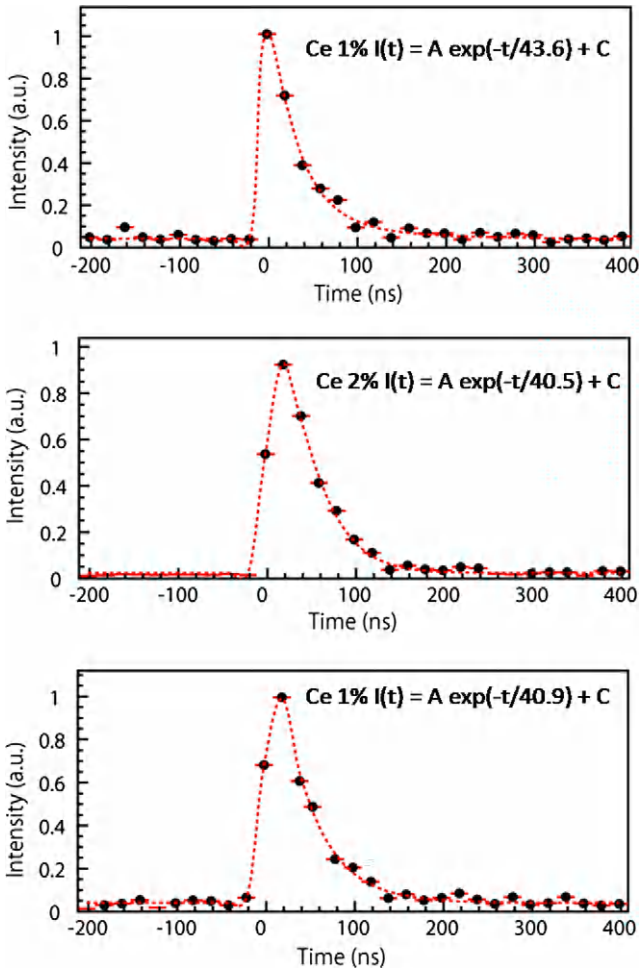

Fig. 7. ^{241}Am α-ray excited decay curves of Ce^{3+} doped LiCAF single crystals. From top to bottom, Ce 1%, 2%, and 3% are shown, respectively. The dotted line represents a fitting function.

Fig. 7 exemplifies decay curves of Ce:LiCAFs. By a single exponential fitting, decay time of Ce 1%, 2%, and 3% turned out to be 44 ns, 41 ns, and 41 ns within a typical error of few ns involving both a fitting and a systematic error of our setup, respectively. Concerning the decay time components, they showed almost the same value with in a typical error. The present result is consistent with our past result (38 ± 1 ns by neutron irradiation [9]) and the other's (35 ± 2 ns by α-ray excitation [11]). The delay of scintillation light, as compared to photoluminescence one, is connected with the energy transfer from host lattice to luminescence centers. Thus, the decay time constants of our Ce:LiCAF are typically twice as fast as that of GS20 (75 ns [6–8]).

4. Conclusions

Ce 1%, 2%, and 3%-doped LiCAF single crystals were grown by the μ-PD method. The crystals were transparent, 2.0 mm in diameter and 40–50 mm in length. Neither visible inclusions nor cracks were observed. Absorption coefficients were in proportional to the nominal Ce concentration. Emission due to Ce^{3+} 5d–4f related transition peaking around 285 nm and 310 nm were observed by 260 nm excitation. Photoluminescence decay times were 26 ns for all the samples. When ^{241}Am was irradiated, the 3% sample showed the highest pulse height and the light yield turned out to be 6600 ph/n after the correction of *QE* of PMT. The α-ray excited decay time constants were around 40 ns for all the crystals.

Acknowledgements

This work was partially supported by Ministry of Ministry of Health and Welfare, Grant-in-Aid for the development of medical instruments. This work was also partially supported by Ministry of Education, Culture, Sports, Science and Technology of Japanese Government, Grant-in-Aid for Young Scientists (A), 19686001 (AY), and a Grant-in-Aid for Young Scientists (B), 15686001 (TY). Partial support of the Yazaki Memorial Foundation for Science and Technology, Japan Science Society, and Iketani Science and Technology Foundation, are also gratefully acknowledged.

References

[1] W. Blanc, C. Dujardin, J.C. Gâcon, C. Pedrini, B. Moine, A.N. Belsky, I. Kamenskikh, M. Kirm, G. Zimmerer, Radiation Effects and Defects in Solids 150 (1–4) (1999) 41.
[2] Carel W.E. van Eijk, NIM-A 471 (1994) 244.
[3] Z. Liu, H. Ohtake, N. Sarukura, M.A. Dubinskii, R.Yu. Abdulsabirov, S.L. Korableva, Nonlinear Optics Apos, vol. 98 (Materials, Fundamentals and Applications Topical Meeting Issue 10–14), 1998, p. 343.
[4] K. Shimamura, S.L. Baldochi, N. Mujilatu, K. Nakano, Z. Liu, H. Ohtake, N. Sarukura, T. Fukuda, Journal of Crystal Growth 211 (2000) 302.
[5] K. Shimamura, N. Mujilatu, K. Nakano, S.L. Baldochi, Z. Liu, H. Ohtake, N. Sarukura, T. Fukuda, Journal of Crystal Growth 197 (1999) 896.
[6] G. Ban, X. Flechard, M. Labalme, T. Lefort, E. Lienard, O. Naviliat, P. Fierlinger, K. Kirch, P. Geltenbort, K. Bodek, in: IEEE NSS MIC 2004 Conference Record, 2004, pp. 829–832.
[7] C.W.E. van Eijk, Radiation Measurements 38 (2004) 337–342.
[8] C.W.E. van Eijk, Radiation Protection Dosimetry 110 (2004) 5–13.
[9] A. Yoshikawa, T. Yanagida, Y. Yokota, N. Kawaguchi, S. Ishizu, K. Fukuda, T. Suyama, K.J. Kim, M. Nikl, M. Miyake, M. Baba, IEEE Transaction of Nuclear Science (2009), accepted for publication.
[10] A. Yoshikawa, T. Satonaga, K. Kamada, H. Sato, M. Nikl, N. Solovieva, T. Fukuda, Journal of Crystal Growth 270 (2004) 427–432.
[11] A.V. Gektin, N.V. Shiran, S.V. Neicheva, M.J. Weber, S.E. Derenzo, W.W. Moses, Journal of Luminescence 102–103 (2003) 460–463.
[12] A. Gektin, N. Shiran, S. Neicheva, V. Gavrilyuk, A. Bensalah, T. Fukuda, K. Shimamura, NIM-A 486 (2002) 274–277.
[13] M. Nikl, N. Solovieva, E. Mihokova, M. Dusek, A. Vedda, M. Martini, K. Shimamura, T. Fukuda, Physica Status Solidi (a) 187 (2001) R1–R3.